BEAM DYNAMICS STUDIES IN THE BEPCII STORAGE RINGS*

Q. Qin#, N. Huang, W.B. Liu, Y.D. Liu, Y.M. Peng, J. Qiu, D. Wang, X.H. Wang, N. Wang, J.Q. Wang, Y.Y. Wei, X.M. Wen, J. Xing, G. Xu, C.H. Yu, C. Zhang, Y. Zhang, Z. Zhao, D.M. Zhou,
IHEP, CAS, P.O. Box 918-9, Beijing 100049, P.R. China

Abstract

As an upgrade project of the Beijing Electron Positron Collider (BEPCII), the commissioning of the storage rings for both collision and synchrotron radiation modes started in Nov. 2006. Besides the normal commissioning on luminosity and beam performance, beam dynamics studies are being carried on as well. Some results on beam parameters determination, single and multi-bunch effect, and beam instabilities of two rings are given in this paper.

INTRODUCTION

The upgrade project of the Beijing Electron Positron Collider (BEPC), BEPCII, is composed of a linac, two transport lines for both positron and electron beams, and two storage rings in parallel to accommodate e- and e+ beams, respectively. The two halves of the outer rings are connected as a synchrotron radiation ring with 14 beam lines extracted from 5 wigglers and 9 bending magnets. The layout and other details of the three rings of BEPCII can be found in [1, 2] in this proceedings.

In this paper, we mainly discuss the beam dynamics study in the collision rings, say, BER and BPR for e- and e+ beam, respectively. Some main nominal parameters of the lattice are listed in Table 1.

Table 1: Main parameters of the BEPCII collision rings

Beam energy	GeV	1.89
Circumference	m	237.53
Beam current	A	0.91
Bunch current / Bunch No.	mA	9.8 / 93
Natural bunch length	mm	13.6
RF frequency	MHz	499.8
Harmonic number		396
Emittance (x/y)	nm.rad	144/2.2
β at IP (x/y)	m	1.0/0.015
Crossing angle	mrad	± 11
Tune (x/y/s)		6.54/5.59/0.034
Momentum compaction		0.0237
Energy spread		5.16×10^{-4}
Natural chromaticity (x/y)		–10.8/–20.8
Luminosity	$cm^{-2}s^{-1}$	1×10^{33}

Figure 1 shows the Twiss functions of the interaction region, the RF region and the whole ring. There're 10 dipoles in each arc of a ring and a quasi-FODO structure with two missing dipoles are applied, in order to have a big emittance and a high beam current.

In the second section, we will discuss the determination of the beam main parameters. Single and multi-bunch beam effects will be introduced in section 3. Some instabilities were observed and showed in section 4. At last, a summary will be given.

*Work supported by National Foundation of Natural Sciences contract 10725525
#qinq@ihep.ac.cn

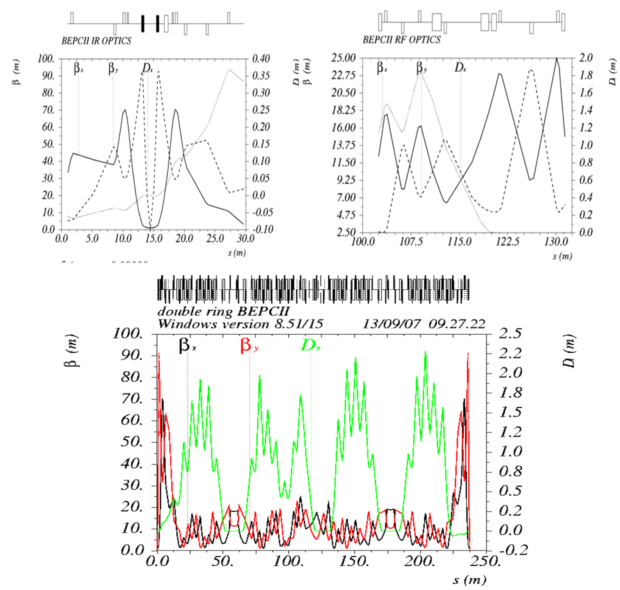

Figure 1: Twiss functions in the IR (up-left), the RF region (up-right) and the whole ring (down) of BER/BPR.

DETERMATION OF BEAM PARAMTERS

β Functions and Transverse Tunes

The beta functions along the two rings are measured before and after the optics corrections with the LOCO [3] based on the measured response matrices. Tune modulation method is applied to measure the beta functions in all the locations of quadrupoles. Figure 2 shows the measured and nominal beta functions after the optics corrections for BER as an example. The relative errors between the nominal and measured beta functions are less then 10% averagely.

The beta functions at the IP are measured with the same

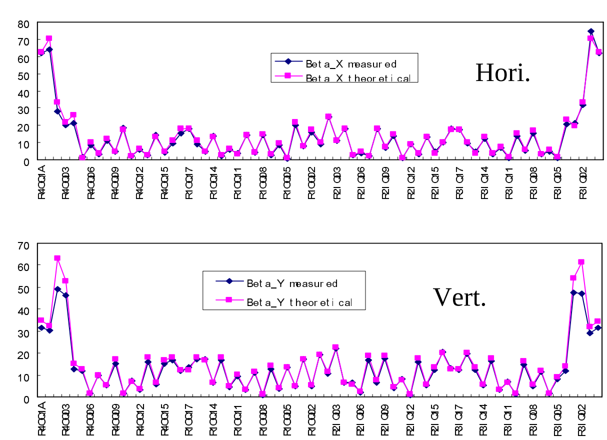

Figure 2: Comparison between measured and nominal β functions in BER after optics correction.

method, but the thick lens model is taken into account as we calculate the average beta at the edge of the first quad near the IP. Since the superconducting quads (SCQ) near the IP off-centrally bend the beam in horizontal, the contribution from this effect is also considered. The average β function of a quad can be expressed as [4]

$$\bar{\beta}_{x,y} = \pm\frac{2}{\Delta kl}\left[\cot(2\pi\nu_{x,y})(1-\cos(2\pi\Delta\nu_{x,y}))+\sin(2\pi\Delta\nu_{x,y})\right], \quad (1)$$

where Δkl means the change of the integral strength of a quad, and $\Delta\nu$ the corresponding change of tunes. If the SCQ bends the beam with an angle of θ, and its bending radius is ρ, we can easily get

$$\bar{\beta}_{x} = \pm\frac{2}{\left(\Delta kl+\frac{\theta}{\rho}\right)}\left[\cot(2\pi\nu_{x})(1-\cos(2\pi\Delta\nu_{x}))+\sin(2\pi\Delta\nu_{x})\right]\cdot \quad (2)$$

The thick lens model [5] of a quad gives us the following formulae to calculate the β functions at the IP, i.e., $\beta_{x,y}^*$ as

$$\begin{aligned}\bar{\beta}_y &= \left\{\frac{L_0\sin^2(k_0l)}{k_0^2 l}+\frac{k_0l-\sin(k_0l)\cos(k_0l)}{2k_0^3 l}+\frac{L_0^2[k_0l+\sin(k_0l)\cos(k_0l)]}{2k_0l}\right\}\cdot\frac{1}{\beta_y^*}\\ &\quad+\frac{k_0l+\sin(k_0l)\cos(k_0l)}{2k_0l}\cdot\beta_y^* \qquad (3)\\ &= C_1\cdot\frac{1}{\beta_y^*}+C_2\cdot\beta_y^*,\end{aligned}$$

and

$$\begin{aligned}\bar{\beta}_x &= \left\{\frac{L_0\sinh^2(k_0l)}{k_0^2 l}-\frac{k_0l-\sinh(k_0l)\cosh(k_0l)}{2k_0^3 l}+\frac{L_0^2[k_0l+\sinh(k_0l)\cosh(k_0l)]}{2k_0l}\right\}\cdot\frac{1}{\beta_x^*}\\ &\quad+\frac{k_0l+\sinh(k_0l)\cosh(k_0l)}{2k_0l}\cdot\beta_x^* \qquad (4)\\ &= D_1\cdot\frac{1}{\beta_x^*}+D_2\cdot\beta_x^*.\end{aligned}$$

Here, k_0l is the nominal integral strength of quad, L_0 is the drift length closest to the IP, and Cs and Ds are connected with $\beta_{x,y}^*$ as

$$\begin{aligned}\beta_y^* &= \frac{\bar{\beta}_y-\sqrt{\bar{\beta}_y^2-4C_1C_2}}{2C_2}\\ \beta_x^* &= \frac{\bar{\beta}_x-\sqrt{\bar{\beta}_x^2-4D_1D_2}}{2D_2}.\end{aligned} \qquad (5)$$

Thus, we can get the $\beta_{x,y}^*$ with the measured average $\beta_{x,y}$ of the SCQs near the IP. The results are listed in Table 2. By anti-symmetrically changing the strengths of SCQs near the IP, the waist of β can be found and thus the $\beta_{x,y}^*$ could be deduced too. The method using LIBERA BPM system to measure the $\beta_{x,y}^*$ is being developed.

Table 2: Measured $\beta_{x,y}$ of the SCQs and the IP

	β_x (m)	β_y (m)
SCQW-1*	1.293	60.87
SCQE-1	3.661	60.60
IP-1	0.983	0.0171
SCQW-2	2.202	62.45
SCQE-2	3.658	62.12
IP-2	0.986	0.0167

* 1 and 2 mean the times of measurement

As listed in [2], the measured tunes are close to the nominal values, since the optics is corrected well.

Dispersion Function

The dispersion functions around the rings are measured with the changing of orbits due to the changing of RF frequency. The results are showed in [3]. From the measured dispersion of the BPMs close to the IP, we can deduce the dispersions at the IP, which are 1 or 2 cm in horizontal and several mm in vertical.

Chromaticity and Optimized RF Frequency

Corrected and natural chromaticities were measured systematically at the first stage of the BEPCII commissioning, in which the SCQs were replaced by the normal conducting magnets. Table 3 shows the results of the chromaticity measurement.

Table 3: Corrected and natural chromaticity measurement

Nomi. ξ_x/ξ_y	Meas. ξ_x/ξ_y	Nomi. ξ_x/ξ_y	Meas. ξ_x/ξ_y
-5.0/-5.0	-5.33/-5.02	-1.0/-1.0	-1.28/-0.82
-3.0/-3.0	-3.19/-2.46	+1.0/+1.0	+1.05/+0.95
-2.0/-2.0	-2.33/-0.89	+5.0/+5.0	+4.50/+3.28
Natural ξ_{x0}/ξ_{y0}	-11.7/-10.4	Meas. ξ_{x0}/ξ_{y0}	-10.33/-10.07

By changing the RF frequency at different chromaticity values, we measured the corresponding transverse tunes, and thus found the central beam path in the sextupoles and the optimized RF frequency, shown in Fig. 3. In the BER, it is 499.802 MHz as that given in Fig. 3.

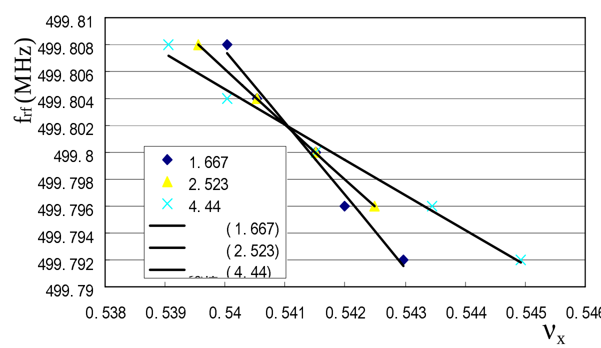

Figure 3: Optimized RF frequency measurement.

Transverse Coupling

The details of the transverse coupling adjustment and measurement are given in [3].

SINGLE BEAM DYNAMICS

Bunch Lengthening

In colliders, bunch lengthening is the main single bunch instability and limits the enhancement of luminosity. After fixing the operation lattice for collision, we measure the bunch lengthening in both rings with streak camera. In the measurement, we use single bunch for each beam without any collision. The momentum compaction is calculated from the measured synchrotron tune and the RF voltage, which was calibrated by the power of cavities. The bunch length is measured when the single bunch current is changed with the fixed RF voltage. The bunch length is fitted with the distribution of bi-Gaussian as that used in the BEPC before [6]. Static image was measured and reduced from the measured bunch lengths. Figure 4 shows the bunch lengthening as a function of current in the BER and BPR, respectively.

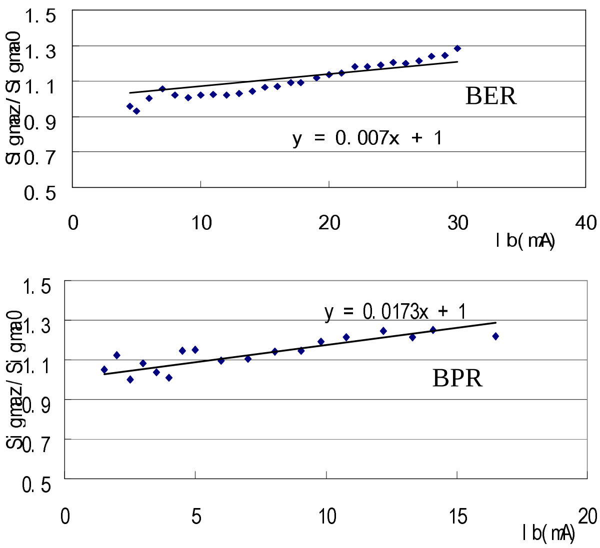

Figure 4: Bunch lengthening vs. bunch current.

From the bunch lengthening, we can get the inductance of the BER and BPR as L = 32.1 nH and L = 118 nH, respectively, which also correspond to $|Z/n|_0$ = 0.25 Ω and $|Z/n|_0$ = 0.94 Ω. Since the bunch lengthens at low current due to potential well distortion, it can be expressed as [7]

$$\frac{\sigma_l}{\sigma_{l0}} \approx 1 + \frac{e\alpha_p I_b \omega_0 L}{8\sqrt{\pi}\nu_s^2 E}\left(\frac{R}{\sigma_{l0}}\right)^3, \qquad (6)$$

where σ_l and σ_{l0} are the bunch length at current I_b and the natural bunch length, respectively, α_p the momentum compaction, ω_0 the angular revolutionary frequency, L the inductance, R the average radius of ring, ν_s the longitudinal tune, and E the beam energy. With the calculated L from the bunch lengthening measurement, we can get $\sigma_l/\sigma_{l0} \approx 0.0053I_b+1$ for the BER and $\sigma_l/\sigma_{l0} \approx 0.01855I_b+1$ for the BPR, respectively, which are similar with the fitting results shown in Fig. 4.

Tune Variation as a Function of Bunch Current

The effective impedance can also be estimated from the tune variation due to the changing of bunch current with the following expressions [8]:

$$\frac{d\nu_\perp}{dI} = \frac{R}{4\sqrt{\pi}(E/e)\sigma_l}\overline{\beta}_\perp Z_{\perp,eff}\ , \qquad (7)$$

where $\overline{\beta}_\perp$ is the average β function around the ring. The tune variation in each ring is got when the bunch current decreases without the other beam existing. Figure 5 shows the results of the measurement. All the measurements are done with single bunch case, and the tunes are measured with the FFT done by the signals taken from the single pass BPM system. With the eq. (6) and $|Z/n|_0=b^2Z_{\perp,eff}/2R$, the estimated low frequency longitudinal impedances of the BER and BPR are $|Z/n|_0$ = 1.29 Ω and $|Z/n|_0$ = 1.10 Ω, respectively. The errors of fitting impedance are less than ±3% after the data filter.

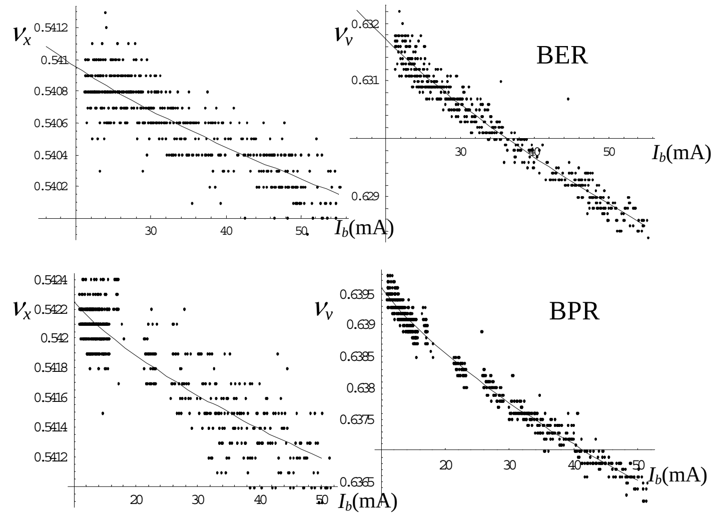

Figure 5: Tune variation as a function of bunch current.

Beam Lifetime

The single bunch beam lifetimes in the BER and BPR are measured for several times under different machine conditions, as shown in Fig. 6. The RF voltage is kept higher than 1.5 MV for enough longitudinal Touschek lifetime during the observations.

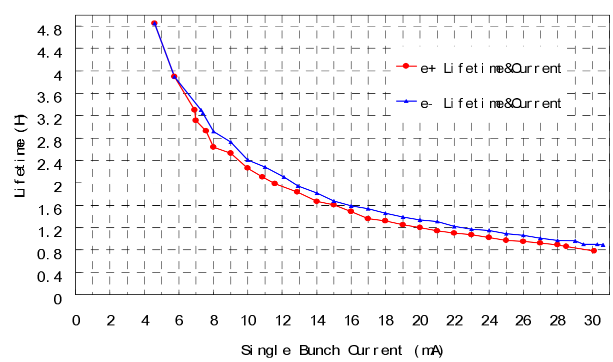

Figure 6: Single bunch beam lifetime observation

From Fig. 6, we can found that at low currents, the lifetime of e- and e+ beam in BER and BPR approaches the same value, which means the Touschek lifetime of the single bunch beam in BER and BPR are the same. By extrapolating the lifetime curve, we get the Touschek lifetime in both rings is about 10 hrs@1mA, which is far from the design value of 7.1 hrs@9.8mA.

With the vacuum pressure given in the rings, the beam-gas lifetime can be estimated. The residual gas consists of about 70% CO and 30% H_2 in the BPR, and 30% CO and 70% H_2 in the BER. At the bunch current of 1mA, the beam-gas lifetime of e+ beam is calculated as 146hrs with the average vacuum pressure is 0.178 nTorr. So the total calculated lifetime of e+ beam is ~43 hrs, which is larger than 10 hrs we observed.

The beam lifetime of multi-bunch case is also observed with different beam currents and vacuum pressure. Figure 7 depicts the average vacuum pressure under different beam current in both rings. Taking an example of 500mA *500mA in collision for both beams, we have the average vacuum pressure of 3.58 nTorr in BPR and 1.79 nTorr in

BER. The various beam lifetimes calculated in both rings and the observed lifetimes are listed in Table 4.

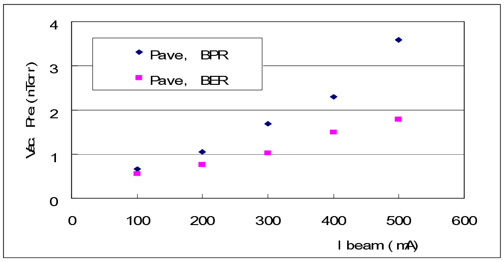

Figure 7: Average vacuum pressure at different beam. current of BER and BPR with same bunch numbers

From Table 4, we can see that the e+ beam lifetime agrees very well to the observed one, while the e- beam doesn't. The reason should be the vacuum is not as good as expected, even at the very low beam current. It is believed that if the vacuum improved, the lifetime at very low bunch current should be longer, which was thought as the Touschek lifetime, and the total beam lifetime would be longer if the Touschek lifetime increased.

Table 4: Calculated and observed (obsd.) beam lifetime

	<p> (nTorr)	b-g (hr)	Tous. (hr)	b-b (hr)	Total (hr)	obsd. (hr)
BER	1.79	33	2.0	6.0	1.44	2.94
BPR	3.58	7.3	2.0	6.0	1.24	1.12

BEAM INSTABILITY

As we discussed previously, bunch lengthening is the main instability of single bunch case in our machine. The electron cloud instability (ECI) becomes the main multi-bunch instability in the positively charged ring, especially the high current factory-like machines. The beam blow-up due to the electron cloud (EC) will cause the reduction of luminosity and the coupled bunch instability will limit the beam current. The ECI was also observed clearly in the BEPCII e+ ring, though the beam current is not as high as other machines. Figure 8 shows the beam spectra we got from both BER and BPR. In Fig. 8, the beam current I_B =

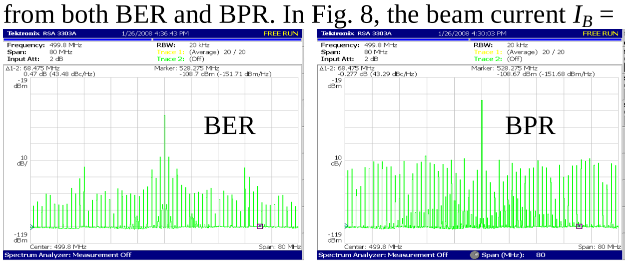

Figure 8: Spectrum distribution of both rings with same I_B.

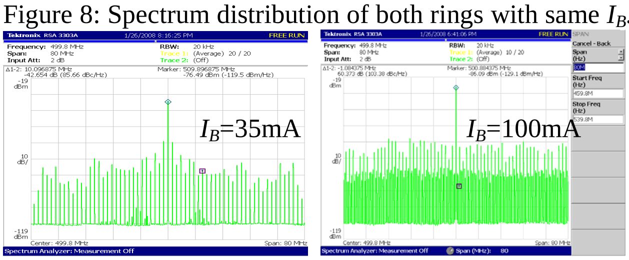

Figure 9: Spectrum in BPR (N_b = 99, uniform filling).

40 mA in both rings with the same bunch pattern. We can easily find that there're more sidebands in BPR than that in BER, which is one of the main evidence of ECI. Keeping the same bunch pattern but changing the bunch current, we can find the threshold beam current of ECI for different bunch numbers, as the example shown in Fig. 9. Table 5 summarizes the threshold we got in the experiment. It seems the threshold current of ECI is low, which is only about two times higher than that in BEPC.

Table 5: Threshold beam current of ECI@different N_b&S_b

N_b	S_b (RF bucket)	I_b (mA)	I_{th} (mA)
48	8	~1.0	~50
99	4	~0.35	~35
198	2	~0.15	~30

The mode distributions got from sidebands analysis are shown in Fig. 10, where we can easily find the difference between the BER and BPR.

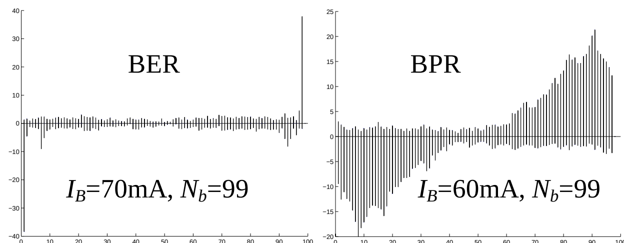

Figure 10: Mode distribution between BER and BPR.

The blow-up of vertical bunch size was also observed with streak camera. We don't find clear blow-up vertically at different bunch pattern and beam current. More studies are needed.

SUMMARY

The BEPCII rings reach their main design parameters after the optics correction in the commissioning. Twiss functions are measured along the rings, and close to the nominal values. The transverse coupling can be adjusted locally with 3 or 4 bumps in sextupoles. Single bunch effects reveal the impedance related issues, and the low frequency longitudinal impedances of the two rings are got from bunch lengthening and tune variation with bunch current. The measured Touschek beam lifetime is far from the calculated one, and thus the total beam lifetime does not agree well enough to the observed one. It could be explained somewhat that the vacuum is not as good as expected right now. ECI has been observed in the e+ ring of BEPCII. The spectra and mode distribution are studied under different bunch patter and current. The threshold current of ECI with 99 uniform filling bunches is about 35 mA. Further studies on beam phenomena are needed.

REFERENCES

[1] C. Zhang, this proceedings, April 2008.
[2] J.Q. Wang, this proceedings, April 2008.
[3] Y.Y. Wei, et al, this proceedings, April 2008.
[4] F. Zimmermann, SLAC-PUB-7844, June 1998.
[5] D.M. Zhou, IHEP-AC-BEPCII/2007-31, 2007.
[6] Q. Qin, et al, NIM A 463 (2001) 77-85.
[7] B. Zotter, CERN 85-19, 1985.
[8] S. A. Heifets and S.A. Kheifets, Rev. Mod. Phys. 63, 631 (1991).